Dynamics of the spontaneous formation of a planar phospholipid bilayer: A new approach by simultaneous electrical and optical measurements

Hisashi Fujiwara,[a] Masayuki Fujihara, and Takashi Ishiwata
Faculty of Information Sciences, Hiroshima City University, 3-4-1 Ozuka Higashi, Asa-minami-ku, Hiroshima 731-3194, Japan

(Received 23 April 2003; accepted 10 July 2003)

An artificial lipid bilayer in planar form, well known as bilayer lipid membrane (BLM), spontaneously forms from a lipid droplet (L-α-phosphatidylcholine in n-decane and chloroform in this work) in an aperture of a thin partition in aqueous solution. The thinning dynamics of the lipid droplet or membrane has been studied by simultaneous capacitance and image recording, because the lipid membrane sandwiched by aqueous solutions can be considered as a parallel-plate capacitor. The simultaneous measurements have revealed the two-step thinning of the lipid membrane from its specific capacitance value: first, the initial droplet thins to yield a membrane of about 100 nm thickness ($0.02\ \mu F/cm^2$), and second, within this thin lipid membrane, a lipid bilayer of 4 nm thickness ($0.42\ \mu F/cm^2$) suddenly emerges and grows, keeping a bilayer structure. In addition, the simultaneous measurements have a time stamp, and thus can determine the trigger moment of the bilayer formation. The revealed dynamics provides the first quantitative support for a ''zipper'' mechanism [H. T. Tien and E. A. Dawidowicz, J. Colloid Interface Sci. **22**, 438 (1966)]; in the mechanism, the first thinning results in a sandwich consisting of the organic solvent between two adsorbed lipid monolayers whose distance is the order of 100 nm, and then a chance contact of both monolayers initiates the formation and growth of a lipid bilayer in a zipper-like manner. However, because of the existence of the two solvent–water interfaces containing surface-active molecules, phospholipids, this work claims that the zipper mechanism should be modified in view of the Marangoni effect. The simultaneous measurements have also revealed the adjacency effect, namely, that only the prebilayer region just adjacent to the bilayer changes into a bilayer. The present formation and growth of a lipid bilayer, including the adjacency effect, can be explained by the classic nucleation theory of two-dimensional crystallization. BLM systems with the simultaneous measurements can be considered as a useful environment for the study of soft-matter chemical physics. © *2003 American Institute of Physics.* [DOI: 10.1063/1.1605372]

I. INTRODUCTION

The phospholipid bilayer is the basic structural unit of biological membranes.[1] Thus, preparation methods of an artificial lipid bilayer are important to construct an experimental model for a variety of biological membranes.[2] Among these methods, extremely simple is the formation of a lipid bilayer in planar form, well known as bilayer or black lipid membrane (BLM) in aqueous solution (Fig. 1).[3] A thin partition or support, usually made of an inert plastic material such as Teflon, is immersed in an electrolyte solution. The support has a small aperture in it, onto which a minute droplet of lipid solution is introduced. Generally, thinning of the lipid droplet occurs spontaneously, and under favorable conditions leads to a lipid bilayer.

A strong advantage of BLM experiments is the high applicability of electrical measurements;[2] insertion of electrodes to both sides of the partition enables the electrical probing of the lipid bilayer. Accordingly, BLM systems have been adopted for studying not only the basic electrical properties[4–7] of lipid bilayers but also more applied subjects such as the photoelectric response of pigmented bilayers[8–11] and the function of ion channels.[12–16] In this manner, most of the BLM experiments have been done in view of biochemistry, biophysics, bioelectronics, and physiology. However, when we focus on the bilayer formation in BLM systems shown in Fig. 1, another important aspect emerges. Namely, initially disordered lipid molecules spontaneously form the ordered bilayer structure, and thus the bilayer formation in BLM systems is an interesting subject in view of the chemical physics of self-assembly.

From such a viewpoint, pioneering investigations have been done by Tien and Dawidowicz.[3,17] They precisely observed the formation process with a low-power microscope in reflected white light ($\lambda > 400$ nm). In the first stage, the lipid droplet thins to yield a ''silvery-golden'' membrane of about 100 nm in thickness. In the second stage, ''black spots'' emerge suddenly, either singly or severally, and grow continuously until they cover the entire aperture except for a peripheral thick region called the Plateau–Gibbs border which connects the microscopic lipid membrane with the macroscopic support.

The black spots have been considered as lipid bilayers because of their color. The black color arises from the de-

[a]Author to whom correspondence should be addressed. Electronic mail: fhisashi@im.hiroshima-cu.ac.jp

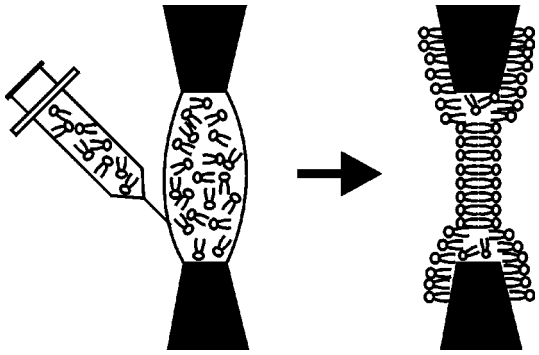

FIG. 1. Preparation method of a bilayer lipid membrane (BLM).

structive interference of the rays reflected from the front and back interfaces of the membrane; the two important factors are a very small optical path difference between both rays and a phase shift of π occurring in the ray reflected from the front interface.[3,17] Therefore, the black color only means that the membrane thickness is much smaller than a quarter wavelength of the white light, and accordingly does not ensure the bimolecular thickness. This situation is well summarized in p. 36 of a famous excellent book by Tien:[3] "*It should be noted that a black or grayish-black lipid membrane may not necessarily be bimolecular or bilayer in thickness*." In the case of the black membrane in steady state, however, the bimolecular thickness has been well confirmed by various measurements including electron microscopy.[3]

To improve this quantitative uncertainty, we note the high applicability of electrical measurements as mentioned above. The planar lipid membrane, regardless of its state (from a droplet to a bilayer), can be treated as a parallel-plate capacitor,[3,4] two good conductors separated by a poor conductor; the electrolyte solutions in both compartments work as a sandwich electrode in close contact with the lipid membrane. The thickness of the lipid membrane d is related to the specific capacitance (capacitance per unit area) of the membrane C_s by

$$d = \varepsilon \varepsilon_0 / C_s, \tag{1}$$

where ε is the relative permittivity of the membrane and ε_0 is the permittivity of vacuum. The specific capacitance can be determined directly by measuring the membrane capacitance and area simultaneously. This type of simultaneous measurements was practically difficult in the 1960s and 1970s, the days of the pioneering investigations. Now, however, such measurements have become easy by virtue of the recent significant progress in computer interfacing and image recording; actually, simultaneous electrical and optical measurements have become an important tool for probing ion channels in BLM.[12,14,16]

In this paper, we describe the first quantitative observation of the spontaneous bilayer formation in BLM systems by the simultaneous capacitance and image recording. We have chosen L-α-phosphatidylcholine as a bilayer-forming lipid, because this phospholipid has been frequently used as a representative one for more than 40 years of BLM experiments. The simultaneous measurements can determine the specific capacitance of the lipid membrane in development

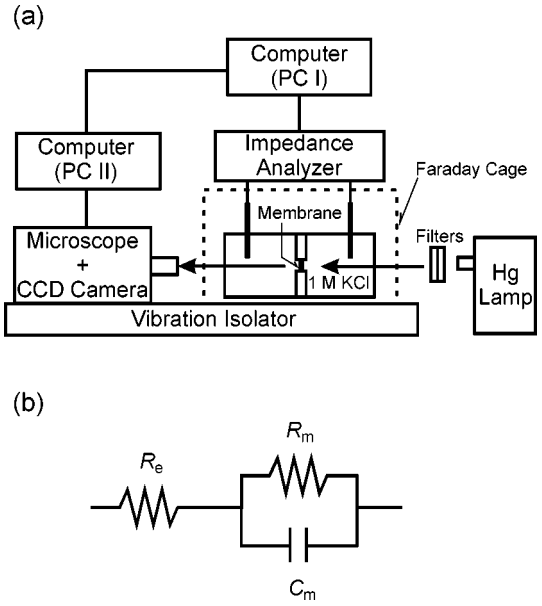

FIG. 2. Schematics of (a) the experimental setup for the simultaneous electrical and optical measurements and (b) an equivalent circuit for the BLM cell.

which directly corresponds to its thickness. The dynamics of the membrane thinning is discussed from two viewpoints, a "zipper" mechanism proposed by Tien and Dawidowicz[3,17] and the classic nucleation theory of two-dimensional crystallization. Consequently, this paper presents a new aspect of BLM systems as a useful environment for the study of soft-matter chemical physics.

II. EXPERIMENT

Figure 2(a) shows the experimental setup for the simultaneous electrical and optical measurements of the bilayer formation. The lipid bilayer was made in an aperture (of diameter ~ 1 mm, but slightly out of round) in a partition of a Teflon cell having two compartments filled with 1 M KCl aqueous solutions. This BLM cell was equipped with two platinized platinum electrodes and two glass windows, and enclosed in a Faraday cage to avoid electromagnetic interferences. The membrane-forming solution was prepared by dissolving L-α-phosphatidylcholine (Sigma P-9671) 100 mg in n-decane 1 ml and chloroform 0.3 ml. This solution was introduced onto the aperture by using a microliter syringe, and the resulting lipid droplet or membrane spontaneously thinned to yield a lipid bilayer.

During the thinning of the lipid membrane, the impedance of the cell, as a parallel combination of capacitance C_p and conductance G_p, was measured with an impedance analyzer (HP4192A, Hewlett Packard) at $f = 10$ kHz, and transferred to a personal computer (PC I). The membrane capacitance C_m equals C_p under the present experimental condition, which is confirmed from the analysis of an equivalent circuit for the BLM cell [see Fig. 2(b)]. This circuit consists of a series combination of electrolyte resistance R_e and membrane impedance, a parallel combination of membrane capacitance C_m and resistance R_m.[3] The relationship between C_m and C_p is given by C_m

$=C_p\{1+2(R_e/R_m)+(R_e/R_m)^2+(\omega R_e C_m)^2\}$, where $\omega=2\pi f$. The terms R_e/R_m and $\omega R_e C_m$ represent a measure of electrolyte conduction compared with that of the membrane. We carefully checked that the value of R_e (80 Ω) was low enough to keep the condition of $R_e/R_m \ll 1$ and $\omega R_e C_m \ll 1$ during the whole thinning process. This condition means that the electrolyte works as a conducting wire and a sandwich electrode in close contact with the membrane, and ensures the relationship of $C_m = C_p$.

On the other hand, simultaneously with the electrical measurement, the lipid membrane was observed vertically on a long-distance microscope with transmitted light. This optical configuration simplifies the area determination of observed objects. The microscope, whose working distance is 12 cm, was equipped with a monochrome charge-coupled device (CCD) camera of 2.1 megapixels (Flovel). The light source was a combination of a 500 W high-pressure mercury lamp, an interference filter (450 nm), and neutral density filters. The membrane images were recorded as a bitmap file on a hard disk drive of another personal computer (PC II) connected to the CCD camera. The contrast of the images was enhanced by using a commercial software after the measurements. The resolution of the images was at least better than 10 μm, which was checked from a clear resolution of 10 μm scale in a calibration slide.

The algorithm of the simultaneous measurements is as follows: PC I sends a measurement-start message to PC II just after recording of a capacitance value, and PC II records an image and then sends a measurement-restart message to PC I. As a result, both electrical and optical data were recorded at 3.6 Hz with a time stamp.

All the measurements were done at room temperature.

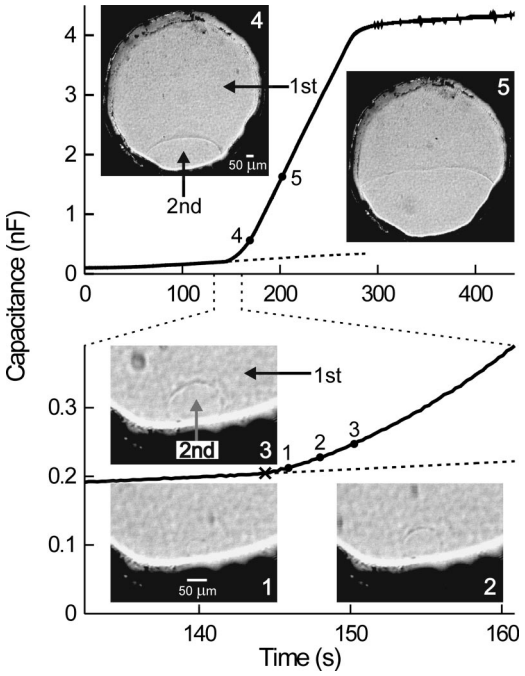

FIG. 3. Capacitance (solid lines) and images (1–5) of a phosphatidylcholine membrane in development. The white lines in images 1 and 4 correspond to 50 μm. The numbered closed circles represent the capacitance values measured simultaneously with the numbered images. In images 3 and 4, the words ''1st'' and ''2nd'' with arrows indicate the first and second regions, respectively. The dashed lines represent the membrane capacitance expected in case of the first thinning continuation without the second thinning. The ''×'' mark represents the trigger moment of the bilayer formation.

III. RESULTS

A. Characteristics of the simultaneous data of the lipid membrane

Figure 3 shows the temporal change of the capacitance and image of the lipid membrane introduced in the cell aperture by applying the membrane-forming solution at 0 s.

First, we summarize the characteristics of the capacitance change. Namely, the membrane capacitance C_m increased with time, first gradually up to 144 s and then steeply until 280 s. This two-stage increase should correspond to the two-stage thinning found previously from the optical observation in reflected light. The latter sudden increase is more apparent in the magnified view, the bottom panel of Fig. 3. The solid line shows the capacitance obtained experimentally, while the dashed line shows an extrapolation of the capacitance values in the first thinning ($C_{1st,ex}$; see the Appendix). Both lines coincide with each other up to the data of 144.4 s indicated by the ''×'' mark, and then they become separate from each other.

Second, we summarize the characteristics of the temporal change of the transmitted image of the lipid membrane (movies 1–3 made from the images obtained from −13 to 274 s are available in EPAPS material).[18] In the first duration of 30 s, the lipid membrane was observed as a transparent bright image containing small particles (or bubbles) moving gradually upward in convectional flow. Then, from 30 until 144 s, three major processes were observed: the formation of the thick peripheral region of the Plateau–Gibbs border, the suction of the membrane inside including the small particles by the Plateau–Gibbs border, and the emergence of a faint shadow region inside the Plateau–Gibbs border. This shadow region, termed ''first region,'' emerged from a lower part of the lipid membrane and grew upward to cover the most of the membrane area inside the Plateau–Gibbs border.

At 144.4 s nothing particular was observed other than the faint first region, but at 145.9 s (image 1 in Fig. 3) a small region was recognized by a boundary consisting of inner bright and outer shadow lines, above a bright curved band corresponding to the Plateau–Gibbs border, in the bottom part of the membrane. This new region, termed ''second region,'' grew in time with progression of the boundary like a blast wave, as can be seen in images 2–5. There exist five image frames between 144.4 and 145.9 s. A reverse-scan animation including these frames (see movie 4 in Ref. 18) reveals that a cloudy object emerges in the first frame (144.6 s) of the five and that in the following four frames it grows into the second region shown in image 1. Therefore, the emergence of the second region coincides with the sudden increase of the membrane capacitance; the trigger moment is determined to be 144.4 s.

The observed first and second regions should correspond to the silvery-golden and black membranes, which will be confirmed in the next section.

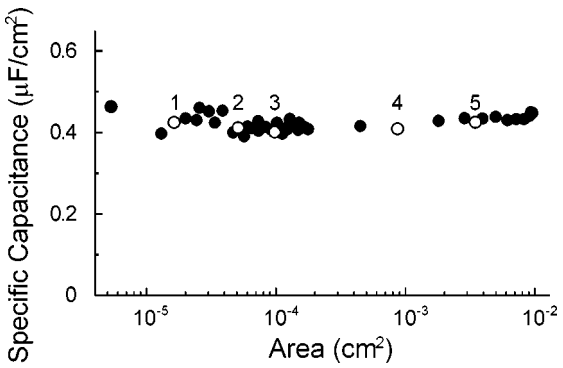

FIG. 4. Specific capacitance of the second region plotted against its area. The numbered open circles represent the data corresponding to the numbered images shown in Fig. 3.

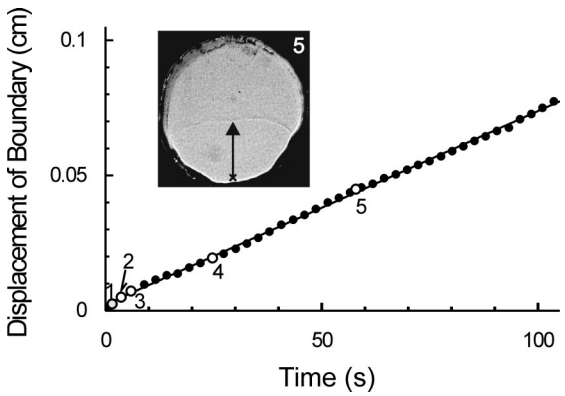

FIG. 5. Analysis of bilayer growth rate. The circles show the vertical displacement of the boundary between the bilayer and prebilayer regions measured from the trigger point of the bilayer formation represented by the "×" mark in image 5; we measured the vertical displacement to minimize the influence of the periphery of the lipid membrane. The zero time is defined as the trigger moment shown in Fig. 3. The numbered open circles represent the data corresponding to the numbered images shown in Fig. 3. The solid line represents a linear fit with the data which corresponds to the speed of 7μm/s.

B. Analysis of the simultaneous data

From both capacitance and image, we can derive the specific capacitance of the lipid membrane (see the Appendix). The specific capacitance is related to the membrane thickness by Eq. (1), where we assume $\varepsilon=2$ based on the reported value for the same phospholipid bilayer in steady state.[4]

Before 144.4 s, we only observed the faint first region, and its specific capacitance $C_{s,1st}$ just before the emergence of the second region is estimated to be 0.02 μF/cm^2. This value corresponds to the thickness of 90 nm, and thus the first region actually corresponds to the silvery-golden membrane observed in reflected light.

After 144.4 s, the second region emerges and grows, and its specific capacitance $C_{s,2nd}$ shows significant characteristics (Fig. 4). The smallest area of the data is 5.3×10^{-6} cm^2 (equivalent with that of a circle of 26 μm diameter), corresponding to the second region observed at 145.2 s. Before this time, it is quite hard to determine the outline of the second region, although its existence is actually confirmed from 144.6 s by the reverse-scan animation. The value of $C_{s,2nd}$ is clearly independent of the area, and its averaged value is 0.42 μF/cm^2. This value corresponds to 4 nm thickness of bilayer one, and is consistent with the steady-state value (0.4 μF/cm^2) reported for the same phospholipid bilayer.[4] Therefore, the simultaneous measurements have confirmed quantitatively, for the first time, that in BLM experiments the suddenly emergent region or spot is actually a lipid bilayer, and also that the emerged bilayer grows with keeping a bilayer structure.

Three additional important characteristics have been extracted from the experiments as follows: (a) Movies 2 and 3 (Ref. 18) of the bilayer formation and growth, together with Fig. 4, indicate the adjacency effect, namely, that only the prebilayer region just adjacent to the bilayer changes into a bilayer. (b) Repetitive observation confirmed that once the bilayer regions emerge either singly or severally (the data in this paper correspond to single emergence), they inevitably grow to cover the whole area inside the Plateau–Gibbs border, the criticality and irreversibility of which are in good agreement with the previous observation in reflected light.[3,17] (c) The bilayer growth rate is constant (Fig. 5), which is also in good agreement with previous reports.[3,17] In our case, however, a concrete value of the growth rate can be easily measured from the simultaneous measurements with a time stamp; several measurements resulted in values in the order of 10 μm/s (e.g., 7 μm/s in Fig. 5).

IV. DISCUSSION

A. Mechanism of the first thinning of the lipid membrane

The simultaneous measurements have shown the dynamics of the first thinning of the lipid membrane, namely, the thinning from the initial droplet to the membrane of about 100 nm thickness, together with both formation of, and suction by, the Plateau–Gibbs border. This dynamics agrees with previous reports,[3,17] and accordingly is explained by the following mechanism proposed in them. After the introduction of the membrane-forming solution, two solvent–water interfaces are formed and then surface-active molecules, phospholipids, migrate to the interfaces orienting themselves with the long-chain hydrocarbon portion immersed in the organic solvent phase. This results in the formation of a phospholipid monolayer in each interface. In parallel with this, the lipid membrane thins to the thickness of about 100 nm by the drainage of the solvent in it. This drainage is mainly due to the gravity (density difference) and the Plateau–Gibbs border suction. Because of the gravitational drainage, the thickness of the lipid membrane decreases from top to bottom inside the Plateau–Gibbs border, which should be the reason for the bilayer emergence in the bottom part of the membrane.[19] The driving force of the Plateau–Gibbs border suction, on the other hand, should be a lower liquid pressure in the Plateau–Gibbs border arising from its high curvature when we consider the Laplace–Young law.[3,20,21]

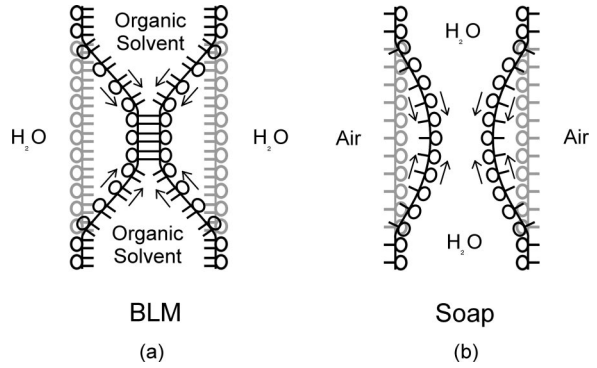

FIG. 6. Structure and dynamics of the interfaces in a BLM system and a soap film. (a) The gray schematic shows the structure of the lipid membrane in the prebilayer state. The black schematic shows tentative bilayer formation and resulting deformation and expansion of the interfaces. (b) The gray schematic shows the structure of an ordinary soap film in air. The black schematics shows local thinning of the soap film and resulting deformation and expansion of the interfaces. In both (a) and (b), arrows represent the motion, in the interfaces, and the adjoining liquid layers, caused by the Marangoni effect.

B. Mechanism of the second thinning of the lipid membrane

The simultaneous measurements have shown, for the first time in quantitative manner, the dynamics of the second thinning of the lipid membrane with the information of its thickness; namely, a lipid bilayer suddenly emerges in the lipid membrane of about 100 nm thickness, and then grows with keeping a bilayer structure. This picture provides the first quantitative support for the zipper mechanism proposed by Tien and Dawidowicz;[3,17] this mechanism has been considered as the most probable one to explain the dynamics of bilayer formation in BLM experiments.[2,22] As described in the previous section, prior to bilayer formation, the lipid membrane has a structure of a sandwich consisting of the organic solvent between two adsorbed monolayers whose distance is the order of 100 nm [the gray schematic of Fig. 6(a)]. They are essentially independent of each other because of the weak van der Waals attractions. However, by some fluctuation such as thermal motion and mechanical vibration, their hydrocarbon chains in a counter configuration can contact each other. Then, the van der Waals attractions between them become strong enough to produce a bilayer of a small area [the black schematic of Fig. 6(a)]. In forming this bilayer, adjacent molecules are drawn close enough to be attracted to the opposite interface. A ''zipper effect'' results, which is responsible for the growth of the lipid bilayer.[3,17]

This zipper mechanism actually explains the two important points of the second thinning, the sudden formation of the lipid bilayer and its growth with keeping a bilayer structure. However, we claim that it should be modified in view of the Marangoni effect,[21,23,24] when we remark that the lipid membrane has two solvent–water interfaces containing surface-active molecules, phospholipids. This structure of the lipid membrane is similar to that of a soap film in air [the gray schematic of Fig. 6(b)];[3,17] a soap film has two water–air interfaces containing surface-active molecules.[20] These types of fluid interfaces adsorbed by surface-active molecules have a resistance to deformation, which is an aspect of what is known as the Marangoni effect, namely, the carrying of bulk material through motions energized by surface (or interfacial) tension gradients.[21]

Imagine a small bilayer is tentatively formed, by a chance contact, within the lipid membrane [the black schematic of Fig. 6(a)]. It accompanies the local deformation and expansion of the interfaces around the bilayer, and the interfacial concentration of the lipid decreases in the deformed region. The resulting interfacial tension gradients, produced by the gradients in lipid concentration, cause a shear stress at the solvent–water interfaces (in the direction of increasing interfacial tension) which induces motion in the interfaces and the adjoining liquid layers.[25] This motion induces a tentative increase of the liquid pressure adjacent to the tentative bilayer and thus works to separate the bilayer into the original monolayers. Namely, the Marangoni effect works as repulsive interaction between the two phospholipid layers of the tentative bilayer. For reference, quite similar rethickening is proposed for a locally thinned region in a soap film [the black schematic of Fig. 6(b)], a phenomenon known as Gibbs elasticity[20] in stabilizing soap films.[24]

In the formation of the tentative bilayer, on the other hand, the repulsive interaction caused by the Marangoni effect should be proportional to the peripheral length of the bilayer, whereas to the bilayer area the net attractive interaction based on both van der Waals attraction and Born repulsion.[3] This qualitative discussion allows us to consider the existence of the critical nucleus size of an emerged bilayer where the two counter interactions are in balance. Once a bilayer larger than this size emerges, it can exist stably and serves as a nucleus for the further bilayer growth. This aspect of BLM experiments, bilayer formation and growth as crystallization, will be discussed in the next section.

Finally, we claim that the Marangoni effect has another counter function of promoting the bilayer growth. Namely, the interfacial flow by the Marangoni effect drags not only the adjoining liquid layers but also the phospholipids themselves to the region just adjacent to the bilayer in growth. Thus, in the case of the stable bilayer larger than the critical size, this flow promotes the phospholipids just around the bilayer to come close to and then contact each other, rather than separate the bilayer. This results in the extension of the bilayer area, and accordingly, the further deformation of the solvent–water interfaces around the extended area. The chain of the phospholipids' contact, interfacial deformation, and interfacial flow proceeds like domino toppling, which is the origin of the zipper effect in the bilayer growth.

C. Bilayer formation and growth as two dimensional crystallization

The consideration of the Marangoni effect, together with both van der Waals attraction and Born repulsion, has suggested the existence of the critical nucleus size in the bilayer formation. This concept can be treated qualitatively by the classic nucleation theory[21,26] of two-dimensional crystallization. The free energy of forming a bilayer disk of radius r containing n phospholipids is the sum of two terms

$$\Delta G = -n\Delta\mu + 2\pi r\gamma, \tag{2}$$

the energy $-n\Delta\mu$ for the transformation of n phospholipids in a prebilayer state to those in a bilayer state, and the peripheral energy $2\pi r\gamma$, where γ is the energy required for making the bilayer periphery of unit length.[27] The first term corresponds to the net attractive interaction based on both van der Waals attraction and Born repulsion, while the second corresponds to the repulsive interaction caused by the Marangoni effect. The number of phospholipids in the bilayer is related to its radius by the equation $n=\rho\pi r^2$, where ρ is the number of phospholipids per unit area.

Taking the derivative of the free energy with respect to radius and setting it equal to zero provides the value of r at the maximum ΔG as $r_c=\gamma/(\rho\Delta\mu)$, which defines the size of the critical nucleus. Then, we write the derivative of the free energy with respect to number in the following form:

$$\frac{d(\Delta G)}{dn}=\left(-1+\frac{r_c}{r}\right)\Delta\mu. \tag{3}$$

This equation defines the free-energy change with one-molecule growth of a bilayer,[28] and is a measure of the driving force of the crystallization. The second term $(r_c/r)\Delta\mu$ represents the peripheral energy increase per one phospholipid incorporation into the bilayer region. This term decreases with a decrease in the curvature $(1/r)$ of the periphery.

The qualitative meaning of Eq. (3) is summarized into the following three cases: (1) $r<r_c$; the free energy increases with the incorporation, because it accompanies substantial increase of the periphery; (2) $r=r_c$; the free energy takes the maximum value which defines the height of the energy barrier; (3) $r>r_c$; the free energy decreases with the incorporation. The combination of these three cases produces the criticality observed in the bilayer formation in BLM experiments, which is explained below.

Before the bilayer formation, case 1 applies to the whole lipid membrane of about 100 nm thickness where the mean thermal energy allows only tentative formation of bilayers smaller than r_c, and they immediately disappear because of the energetic disadvantage caused by the Marangoni effect.

At a certain moment, however, some favorable fluctuation can overcome the energy barrier defined in case 2 and results in the formation of a stable nucleus, a bilayer larger than r_c, at a certain position. It dramatically changes the situation since then; case 3 applies to the whole lipid membrane around the nucleus. The bilayer growth becomes a favorable process, and after a while it reaches the condition of $r\gg r_c$. This condition means, in the scale of phospholipid molecules, that the progress of the periphery with the bilayer growth can be treated as that of a plane wave. Thus, in a good approximation, the condition corresponds to the bilayer growth without substantial increase of the periphery. With these backgrounds, a re-viewing of movie 2 (Ref. 18) of the bilayer growth provides a vivid picture: the arrival of the periphery with a small or negligible curvature strongly reduces or nulls the energy barrier, which is the origin of both irreversibility and adjacency effect.

With the condition of $r\gg r_c$, on the other hand, Eq. (3) gives the constant value of $-\Delta\mu$, indicating the constant driving force of the bilayer growth. Therefore, in this stage, the constant growth rate is expected to be observed, which is surely the case for the present experimental data shown in Fig. 5. Thus, unfortunately, the present image recording only covers the steady-state growth. In other words, the radius of the critical nucleus r_c should be much smaller than the present image resolution; possible improvements of the image resolution will be discussed in the next section.

The concept of two-dimensional crystallization[29] in BLM experiments has been proposed intuitively,[3] and is addressed, for the first time, by the simultaneous measurements. We claim that this work provides an example of two-dimensional crystallization in the strict sense; the present crystallization is strictly two-dimensional without a substrate of a crystal surface.

D. Optical observation of the lipid membrane in transmission illumination

In view of optics, the structure of the lipid membrane during the bilayer growth is interesting. The thicknesses of both bilayer and prebilayer regions are different from each other (4 nm and about 100 nm, respectively). Both regions are essentially transparent, but their refractive indices should be different from each other, reflecting their differences in physical structure. Thus, the lipid membrane is considered as a phase object; the phase object[30–33] is defined as a completely transparent object which, however, has an optical thickness varying from point to point.

In transmission illumination, image contrast of a phase object commonly arises from the Becke lines introduced by refraction at object boundaries that are slightly out of focus.[32] In the present case, as shown in the images of Fig. 3, the bilayer region is distinguished from the prebilayer region by a boundary consisting of inner bright and outer shadow lines. These lines should be the Becke lines, although we did not intend a defocus condition. The long-distance microscope inherently has a low numerical aperture (NA), which should be the reason for the appearance of the Becke lines.[32]

To achieve better image resolution, however, the value of NA should be increased in exact focus, and thus we cannot expect Becke lines to form image contrast. This is a typical conflict between contrast and resolution,[31] commenced in optical observation of a phase object in transmission illumination. However, for the formation of in-focus, high-resolution images of phase objects, both phase-contrast and interference-contrast microscopes were developed in the 20th century.[31] Thus, now we consider the use of them to detect the critical nucleus of the bilayer formation, although we cannot exclude the possibility that the size of the critical nucleus is smaller than the ultimate resolution (100–200 nm) of optical microscopes.[31] Even in this unfavorable case, however, the lipid membrane during the bilayer growth should be an interesting object for both microscopes.

E. New aspect of BLM experiments in view of soft-matter chemical physics

BLM experiments provide a useful environment for studying spontaneous formation of a phospholipid bilayer, in other words, self-assembly of phospholipids. In BLM experi-

ments, bilayer formation proceeds within the well-defined space, the inside of the aperture, and thus can be observed both directly and dynamically by optical microscopy. Furthermore, by virtue of the electrolyte as a conducting wire and a sandwich electrode, bilayer formation can be probed, again both directly and dynamically, by electrical measurement. The resultant applicability of the simultaneous measurements is a unique advantage of BLM experiments, when compared with the other bilayer formation methods such as various liposome preparations.[2,34] In particular, as shown in this paper, the simultaneous measurements can determine the trigger moment of the bilayer formation, and thus provide a concrete possibility of investigating this moment precisely (e.g., the detection of the critical nucleus bilayer). We emphasize this point, because the essence of self-assembly should be included in the moment of a new structure formation.

This work has shown other two points of BLM experiments: the bilayer formation and growth can be considered as two-dimensional crystallization, and they should include the dynamics of an interface containing surface active molecules (e.g., the Marangoni effect). These two points and the first point, self-assembly of phospholipids, correspond to important subjects of soft-matter chemical physics, namely, phase transition, interface activity, and structural organization, respectively.[35,36] The simultaneous electrical and optical measurements open new possibilities of treating these subjects in BLM systems, which is a new aspect of BLM experiments.

ACKNOWLEDGMENTS

The authors thank A. Tamura and K. Tatibana for technical assistance. We also thank N. Happo and J. Kohda for discussions. H.F. thanks K. Yoshida for help in the manuscript preparation. H.F. was supported by a Grant-in-Aid for Encouragement of Young Scientists (No. 12780501) from the Ministry of Education, Science, Sports and Culture, Japan. H.F. was also supported by the Sasagawa Scientific Research Grant from The Japan Scientific Society and a Hiroshima City University Grant for Special Academic Research (General Studies).

APPENDIX: DERIVATION OF THE SPECIFIC CAPACITANCE

This section shows how to derive the specific capacitance of the lipid membrane from both capacitance and image. For this purpose, the following three physical values are obtained from the simultaneous data: the whole membrane capacitance C_m and the areas of the first and second regions, S_{1st} and S_{2nd}. From a notational reason we introduce an area of the thin membrane part S_m $(=S_{1st}+S_{2nd})$ defined as a membrane area inside the Plateau–Gibbs border. This thin membrane part only contributes to C_m, because the contribution of the Plateau–Gibbs border can safely be neglected.[3]

In the fist thinning, the first region only exists and grows, and thus the specific capacitance $C_{s,1st}$ can be derived simply by $C_{s,1st}=C_m/S_m$ $(C_m=C_{1st}$ and $S_m=S_{1st})$.

In the second thinning, however, both first and second regions coexist and thus an essential problem should be treated; the capacitance value originally has no spatial resolution. The membrane capacitance C_m consists of the parallel combination of C_{1st} and C_{2nd}, namely $C_m=C_{s,1st}S_{1st}+C_{s,2nd}S_{2nd}$, where $C_{s,2nd}$ is the specific capacitance of the second region. A solution of this problem is to estimate the $C_{s,1st}$ value in the second thinning. A simple approximation, the use of the $C_{s,1st}$ value just before the emergence of the second region, is inappropriate in the present case, because, even in the second thinning, the growth of the first region, which corresponds to the increase of S_m, gradually proceeds in the upper part of the lipid membrane. Therefore, as a better approximation, we assume that the first region grows independently of the second region which grows from the lower part, and that the $C_{s,1st}$ value in the second thinning can be estimated by an extrapolation of that in the first thinning. In practice, for 90–140 s, we obtain an empirical equation of C_m $(=C_{1st})$ as a function of S_m $(=S_{1st})$. We extrapolate this equation to S_m in 140–300 s; this extrapolation $C_{1st,ex}$ (the dashed lines in Fig. 1) is also used to determine the trigger moment of the bilayer formation from the capacitance change as described in the text. Consequently, we obtain $C_{s,1st}=C_{1st,ex}/S_m$ and then $C_{s,2nd}=(C_m-C_{1st,ex})/S_{2nd}+C_{1st,ex}/S_m$.

[1] H. Lodish, D. Baltimore, A. Berk, S. L. Zipursky, P. Matsudaira, and J. Darnell, *Molecular Cell Biology*, 3rd ed. (W. H. Freeman, New York, 1995).
[2] H. T. Tien and A. Ottova, *Membrane Biophysics* (Elsevier Science, Amsterdam, 2000).
[3] H. T. Tien, *Bilayer Lipid Membranes (BLM): Theory and Practice* (Dekker, New York, 1974).
[4] T. Hanai, D. A. Haydon, and J. Taylor, Proc. R. Soc. London, Ser. A **281**, 377 (1964).
[5] T. Hanai, D. A. Haydon, and J. Taylor, J. Theor. Biol. **9**, 278 (1965).
[6] S. H. White, Biophys. J. **10**, 1127 (1970).
[7] J. P. Dilger, S. G. A. McLaughlin, T. J. McIntosh, and S. A. Simon, Science **206**, 1196 (1979).
[8] H. T. Tien, Nature (London) **219**, 272 (1968).
[9] H.-M. Ullrich and H. Kuhn, Biochim. Biophys. Acta **266**, 584 (1972).
[10] J. S. Huebner, J. Membr. Biol. **39**, 97 (1978).
[11] H. Fujiwara and Y. Yonezawa, Nature (London) **351**, 724 (1991).
[12] Y. Hanyu, T. Yamada, and G. Matsumoto, Biochemistry **37**, 15376 (1998).
[13] G. Basañez, A. Nechushtan, O. Drozhinin, A. Chanturiya, E. Choe, S. Tutt, K. A. Wood, Y.-T. Hsu, J. Zimmerberg, and R. J. Youle, Proc. Natl. Acad. Sci. U.S.A. **96**, 5492 (1999).
[14] T. Ide and T. Yanagida, Biochem. Biophys. Res. Commun. **265**, 595 (1999); T. Ide, Y. Takeuchi, and T. Yanagida, Single Mol. **1**, 33 (2002).
[15] S. Amemiya and A. J. Bard, Anal. Chem. **72**, 4940 (2000).
[16] V. Borisenko, T. Lougheed, J. Hesse, E. Füreder-Kitzmüller, N. Fertig, J. C. Behrends, G. A. Woolley, and G. J. Schütz, Biophys. J. **84**, 612 (2003).
[17] H. T. Tien and E. A. Dawidowicz, J. Colloid Interface Sci. **22**, 438 (1966).
[18] See EPAPS Document No. E-JCPSA6-119-711337 for movies of the lipid membrane in development (from −13 to 143 s for movie 1, from 143 to 274 s for movie 2, and from 143.1 to 153.3 s as a magnified view for movie 3) and a reverse-scan animation of the simultaneous data from 143.1 to 153.3 s (movie 4). A direct link to this document may be found in the online article's HTML reference section. The document may also be reached via the EPAPS homepage (http://www.aip.org/pubservs/epaps.html) or from ftp.aip.org in the directory /epaps/. See the EPAPS homepage for more information.
[19] From repetitive observation, the bilayer emerges not always but mostly in the bottom part.
[20] P. Walstra, in *Foams: Physics, Chemistry and Structure*, edited by A. J. Wilson (Springer, Berlin, 1989); D. Weaire and S. Hutzler, *The Physics of Foams* (Oxford University Press, Oxford, 1999).

[21] A. W. Adamson and A. P. Gast, *Physical Chemistry of Surfaces*, 6th ed. (Wiley, New York, 1997).
[22] H. T. Tien, R. H. Barish, L.-Q. Gu, and A. L. Ottova, Anal. Sci. **14**, 3 (1998).
[23] C. V. Sternling and L. E. Scriven, AIChE J. **5**, 514 (1959).
[24] L. E. Scriven and C. V. Sternling, Nature (London) **187**, 186 (1960).
[25] S. M. Troian, X. L. Wu, and S. A. Safran, Phys. Rev. Lett. **62**, 1496 (1989).
[26] Y. Saito, *Statistical Physics of Crystal Growth* (World Scientific, Singapore, 1996).
[27] The energy γ corresponds to surface tension of a three-dimensional crystal; the periphery of the bilayer disk can be considered as ''surface'' of the two-dimensional crystal.
[28] We obtain Eq. (3) even when we start with a modified Eq. (2), $\Delta G = -n\Delta\mu + r\theta\gamma$, for a sector with a central angle θ in the disk where $n = \rho r^2\theta/2$. Equation (3) is certainly applicable to the present bilayer growth when we postulate an appropriate value of θ; for example, the postulation of a sufficiently small θ is appropriate for the treatment of the vertical displacement shown in Fig. 5.
[29] From a different viewpoint, the formation and growth of a bilayer in BLM experiments may also be considered as dewetting, a phenomenon which, in some instances, proceeds from hole formation as a nucleation process (see p. 468 of Ref. 21). In the gray schematic of Fig. 6(a), we may consider that the organic solvent film exits between two surfaces consisting of the tails of the hydrocarbon chains. Then, the tentative bilayer formation [the black schematic of Fig. 6(a)] corresponds to the hole formation.
[30] R. S. Longhurst, *Geometrical and Physical Optics*, 3rd ed. (Longman Scientific & Technical, Essex, 1973).
[31] E. M. Slayter and H. S. Slayter, *Light and Electron Microscopy* (Cambridge University Press, Cambridge, 1992).
[32] S. Inoue and R. Oldenboug, in *Handbook of Optics*, 2nd ed., edited by M. Bass, E. W. V. Stryland, D. R. Williams, and W. L, Wolfe (McGraw-Hill, New York, 1995), Vol. II.
[33] S. Bradbury and P. Evennett, *Contrast Techniques in Light Microscopy* (BIOS Scientific, Oxford, 1996).
[34] R. R. C. New, in *Liposomes as Tools in Basic Research and Industry*, edited by J. R. Philippot and F. Schuber (CRC, Boca Raton, 1995).
[35] S. A. Safran, *Statistical Thermodynamics of Surfaces, Interfaces, and Membranes* (Perseus, Reading, 1994).
[36] Ian W. Hamley, *Introduction to Soft Matter—Polymers, Colloids, Amphiphiles and Liquid Crystals* (Wiley, New York, 2000).